# Fluxionality and Isomerism of the Bis(dihydrogen) Complex $RuH_2(H_2)_2(PCy_3)_2$: INS, NMR, and Theoretical Studies

**Venancio Rodriguez, Sylviane Sabo-Etienne, and Bruno Chaudret***

Laboratoire de Chimie de Coordination du CNRS, 205 Route de Narbonne, 31077 Toulouse Cedex 4, France

**John Thoburn, Stefan Ulrich, and Hans-Heinrich Limbach**

Institut für Organische Chemie, Fachbereich Chemie, Freie Universität Berlin, Takustrasse 3, D-14195 Berlin 33, Germany

**Juergen Eckert**

Manuel Lujan, Jr., Neutron Scattering Center (LANSCE), Los Alamos National Laboratory, Los Alamos, New Mexico 87545

**Jean-Claude Barthelat, Khansaa Hussein,† and Colin J. Marsden**

Laboratoire de Physique Quantique, UMR IRSAMC-CNRS UMR 5626, Université Paul Sabatier, 118 Route de Narbonne, 31062 Toulouse Cedex 4, France

*Received June 5, 1997*

To study the fluxionality of the bis(dihydrogen) complex $RuH_2(H_2)_2(PCy_3)_2$ (**1**), NMR spectra were recorded in Freons (mixture of $CDCl_3$, $CDFCl_2$, and $CDF_2Cl$). **1** was found to remain fluxional at all temperatures, but the presence of $CDCl_3$ necessary for its solubilization induces its transformation into, first, $RuHCl(H_2)_2(PCy_3)_2$ (**3**) and the new ruthenium(IV) dihydride $RuH_2Cl_2(PCy_3)_2$ (**4**). **4** is produced selectively in pure $CDCl_3$ but reacts further to give a mixture of chloro complexes. **4** was isolated from the reaction of **1** with aqueous HCl in $Et_2O$ and shows a fluxional process attributed to the interconversion between two symmetrical isomers. The activation parameters of this process were obtained by $^1H$ NMR line shape analysis, as well as those corresponding to the exchange between **3** and free dihydrogen. The fluxionality of the dihydrogen−hydride system is also evident at a much faster time scale than that of NMR studies in the inelastic neutron scattering observations of the rotation of the dihydrogen ligands. The geometries and relative energies of several isomers of complexes **1**, **3**, and **4** were studied using density functional theory (DFT) and MP2 methods, together with a few coupled-cluster (CCSD(T)) calculations. In contrast to what might have been expected, the two hydrides and the two $H_2$ units of **1** lie in the same plane, due to the attractive "cis effect" created by the hydrides. The two $H_2$ ligands adopt cis positions in the lowest-energy isomer. Rotation of the two dihydrogen ligands has been analyzed using DFT calculations. A slight preference for a $C_2$ conrotatory pathway has been found with a calculated barrier in good agreement with the experimental INS value. Two low-energy isomers of **4** have been characterized computationally, both of which have $C_{2v}$ symmetry, consistent with the solution NMR spectra.

## 1. Introduction

The discovery by Kubas of dihydrogen coordination without dissociation has opened a whole new field in inorganic chemistry[1−5] and stimulated a renewed interest in polyhydride chemistry. The complex $RuH_2(H_2)_2(PCy_3)_2$ (**1**)[6] has long been the only reported thermally stable bis(dihydrogen) complex, until the recent characterization of $LRuH(H_2)_2$ (L = HB(3,5-$Me_2$-pz), HB(3-$^i$Pr-4-Br-pz)[7] and of $[OsH_3(H_2)_2(P^iPr_3)_2]^+$,[8] respectively, by our group and Caulton and Tilset. Other bis(dihydrogen) complexes have either been prepared in a matrix[9] or observed in solution.[10]

A striking feature of most hydrido dihydrogen complexes is

† Permanent address: Department of Chemistry, Faculty of Sciences, University Al-Baath, Homs, Syria.

(1) Kubas, G. J. *Acc. Chem. Res.* **1988**, *21*, 120.
(2) (a) Crabtree, R. H.; Hamilton, D. G. *Adv. Organomet. Chem.* **1988**, *28*, 295. (b) Crabtree, R. H. *Acc. Chem. Res.* **1990**, *23*, 95. (c) Crabtree, R. H. *Angew. Chem., Int. Ed. Engl.* **1993**, *32*, 789.
(3) Jessop, P. G.; Morris, R. H. *Coord. Chem. Rev.* **1992**, *121*, 155.
(4) Heinekey, D. M.; Oldham, W. J., Jr., *Chem. Rev.* **1993**, *93*, 913.
(5) Burdett, J. K.; Eisenstein, O.; Jackson, S. A. In *Transition Metal Hydrides: Recent Advances in Theory and Experiment*; Dedieu, A., Ed.; VCH: New York, 1991; p 149.
(6) (a) Chaudret, B.; Poilblanc, R. *Organometallics* **1985**, *4*, 1722. (b) Arliguie, T.; Chaudret, B.; Morris, R. H.; Sella, A. *Inorg. Chem.* **1988**, *27*, 598.
(7) Moreno, B.; Sabo-Etienne, S.; Chaudret, B.; Rodriguez, A.; Jalon, F.; Trofimenko, S. *J. Am. Chem. Soc.* **1995**, *117*, 7441.
(8) Smith, K.-T.; Tilset, M.; Kuhlman, R.; Caulton, K. G. *J. Am. Chem. Soc.* **1995**, *117*, 9473.

S0020-1669(97)00697-6 CCC: $15.00 
Published on Web 06/19/1998

**Chart 1**

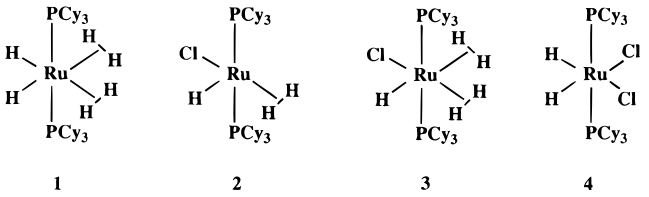


their fluxionality leading to the observation of a single peak in $^1$H NMR at all usual temperatures whenever a hydride is located cis to a dihydrogen ligand.[2−4] This is in particular the case for **1**. Only a few static spectra have been reported for such complexes.[11] However, Freon solvents can give access to a much larger temperature range down to ca. 130 K. Since infrared data were clearly in agreement with a *cis*-dihydride structure, we have investigated the NMR properties of **1** at very low temperature.

We have studied for several years the reactivity of **1**, and for example, we have previously reported the reactions of **1** with halocarbons yielding novel 16-electron dihydrogen derivatives.[12] However, during the course of this work, we found that **1** reacts with chloroform to yield a new unstable ruthenium(IV) dihydride. A very similar complex, namely $RuH_2Cl_2(P^iPr_3)_2$, was recently reported by Werner and co-workers.[13]

In addition, one of us has developed the use of INS for the determination of the rotation barrier of dihydrogen ligands.[14] This rotation barrier can provide information on the mode of coordination of dihydrogen and possible interactions with nearby hydrides.

We describe in this paper an INS study in the solid state, an NMR study of **1** in Freons, and a study of the reactivity of **1** with chloroform leading to a new ruthenium(IV) dihydride complex **4**. Theoretical studies of several possible isomers of **1** are reported, and the concerted rotation of the two dihydrogen ligands is analyzed. Isomers of **4** are also studied computationally.

## 2. Inelastic Neutron Scattering Studies on $RuH_2(H_2)_2(PCy_3)_2$

Data collected on $RuH(H_2)I(PCy_3)_2$ at various incident neutron wavelengths failed to reveal any low-frequency rotational tunneling transitions for the dihydrogen ligand. On the basis of the known energy resolution of the spectrometer for the longest incident wavelength used, we can place a lower limit on the barrier to rotation for $H_2$ in this compound of approximately 2.5 kcal/mol, given that the $d$(HH) is 1.03 Å from X-ray diffraction.[12a]

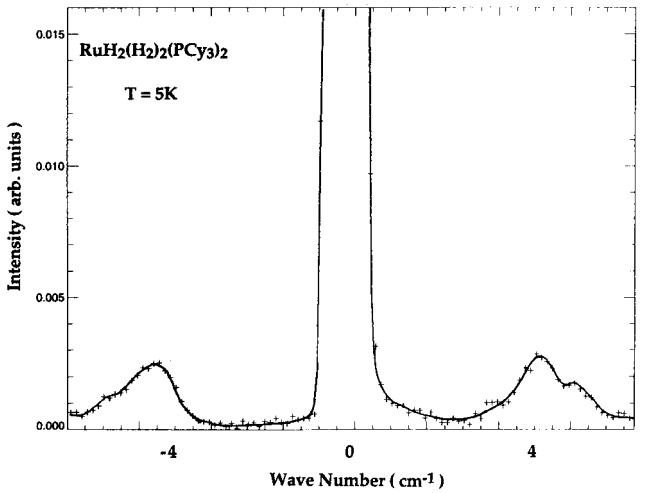


**Figure 1.** Inelastic neutron scattering spectrum of $RuH_2(H_2)_2(PCy_3)_2$ at $T = 5$ K collected on the IN5 spectrometer at ILL with an incident wavelength of 6 Å.

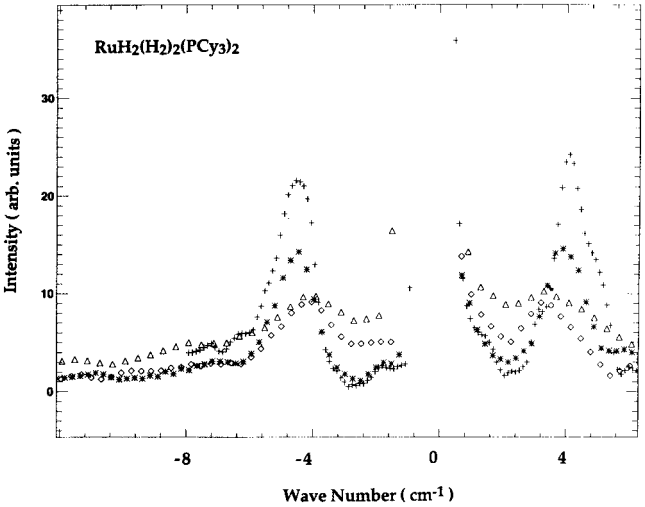


**Figure 2.** Temperature dependence of the INS spectrum of $RuH_2(H_2)_2(PCy_3)_2$: 5 K (+); 50 K (*); 75 K (△); 100 K (◇).

At temperatures below 50 K, the INS spectrum of **1**, on the other hand, consists of the usual pair of bands from the rotational transitions within the librational ground state at ±4.7 cm$^{-1}$. These can be interpreted in terms of planar rotation in a double-minimum potential well[14a] to yield a barrier to rotation of 1.1 kcal/mol. The structure which is evident in these bands (Figure 1) is noteworthy when compared with rotational tunneling lines of other dihydrogen complexes (Figure 4 in ref 14a). It may indicate that there are at least two inequivalent dihydrogen ligands in the solid or be the result of interactions between the two dihydrogen ligands. In view of fluxionality and the computational results described below, we are inclined to attribute this observation to the latter possibility.

As the temperature is increased (Figure 2), the tunneling peaks shift to lower energy and broaden in the usual manner where the width shows an Arrhenius type temperature dependence with an apparent activation energy of about 0.4 kcal/mol. In addition, a broad quasielastic feature appears below the inelastic peaks at temperatures above 75 K. The rotational tunneling peaks coalesce into a broad quasielastic line below the elastic peak above 150 K (Figure 3). The width of this line continues to increase with temperature up to 250 K, the highest temperature reached in this experiment. The activation energy derived from the temperature dependence of the width of this quasielastic

(9) (a) Sweany, R. L. *J. Am. Chem. Soc.* **1985**, *107*, 2374. (b) Upmacis, R. K.; Poliakoff, M.; Turner, J. J. *J. Am. Chem. Soc.* **1986**, *108*, 3645.
(10) (a) Crabtree, R. H.; Lavin, M. *J. Chem. Soc., Chem. Commun.* **1985**, 1661. (b) Michos, D.; Luo, X.-L.; Faller, J. W.; Crabtree, R. H. *Inorg. Chem.* **1993**, *32*, 2, 1370. (c) Fontaine, X. L R.; Fowles, E. H.; Shaw, B. L. *J. Chem. Soc., Chem. Commun.* **1988**, 482.
(11) (a) Crabtree, R. H.; Lavin, M.; Bonneviot, L. *J. Am. Chem. Soc.* **1986**, *108*, 4032. (b) Bianchini, C.; Perez, P. J.; Peruzzini, M.; Zanobini, F.; Vacca, A. *Inorg. Chem.* **1991**, *30*, 279.
(12) (a) Chaudret, B.; Chung, G.; Eisenstein, O.; Jackson, S. A.; Lahoz, F.; Lopez, J. A. *J. Am. Chem. Soc.* **1991**, *113*, 2314. (b) Christ, M. L.; Sabo-Etienne, S.; Chaudret, B. *Organometallics* **1994**, *13*, 3800. (c) Sabo-Etienne, S.; Chaudret, B. *Coord. Chem. Rev.* In press.
(13) Grünwald, C.; Gevert, O.; Wolf, J.; Gonzalez-Herrero, P.; Werner, H. *Organometallics* **1996**, *15*, 1960.
(14) (a) Eckert, J.; Kubas, G. J. *J. Phys. Chem.* **1993**, *97*, 2378. (b) Limbach, H.-H.; Ulrich, S.; Buntkowsky, G.; Sabo-Etienne, S.; Chaudret, B.; Kubas, G. J.; Eckert, J. *J. Am. Chem. Soc.* In press.

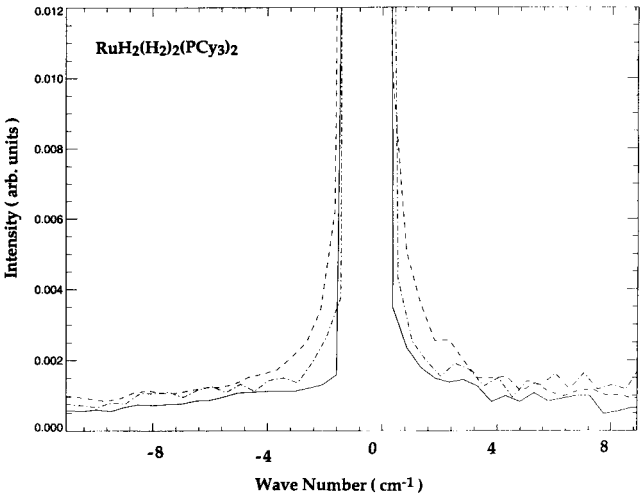


**Figure 3.** Quasielastic scattering from $RuH_2(H_2)_2(PCy_3)_2$ at $T = 150$ K (—), 200 K (— · —), and 250 K (- - -).

line is about 0.25 kcal/mol, which suggests that the motion giving rise to this line may be described[15] as weakly hindered rotational diffusion of dihydrogen. In addition, a second, more narrow quasielastic component is evident at 250 K with a fwhm of approximately 4 $cm^{-1}$.

The increase in width of the rotational tunneling transition lines as a function of temperature is the result of inhomogeneous broadening from coupling to the phonon bath and of the incoherent dihydrogen exchange processes as we recently described.[14b] The value of the activation energy for the inhomogeneous broadening of the tunneling line (0.4 kcal/mol, or 140 $cm^{-1}$) is expected[16] to be similar to the librational transition (torsion) which is responsible for the coupling to the phonon bath in this model. The torsion can be calculated to be 180 $cm^{-1}$ for the present case with a simple 2-fold rotational potential. This is in fair agreement with the prediction of this model[16] whereby the remaining discrepancy may indicate the neglect of other processes such as the incoherent dihydrogen−hydride exchange.

The observed non-Arrhenius behavior (i.e., the two different activation energies for different temperature regimes reported above) is also consistent with the superposition of inhomogeneous broadening from coupling to the phonon bath and of the incoherent dihydrogen exchange processes. Moreover, it is interesting to note that, at the temperature at which the rotational tunneling lines coalesce into a quasielastic line, i.e around 150 K, the NMR data demonstrate the existence of rapid intramolecular hydrogen exchange even though the activation energy for the latter process is much higher than those observed by INS for the rotational motions. This may suggest that the rotational motions of dihydrogen observed by INS are apparently affected by the presence of the dihydrogen−hydride exchange. One may then assume that, in the course of this interconversion of hydride and dihydrogen ligands, the latter can occur in a variety of environments in addition to that of the octahedral coordination sites. These considerations would account for the INS observations at 75 and 100 K, i.e., that the relatively sharp rotational tunneling bands arise from rotational transitions of dihydrogen located in their well-defined potential wells while the broad quasielastic component below the rotational tunneling peaks may be attributed to dihydrogen affected by the rapid intramolecular exchange of hydride and dihydrogen ligands.


**Figure 4.** 500 MHz $^1H$ NMR spectra of **1** dissolved in a mixture of deuterated Freons ($CDCl_3$:$CDFCl_2$:$CDF_2Cl$ = 1:5:5) as a function of temperature. For assignment see text.

### 3. NMR Studies of 1 in a Freon Mixture

To gain additional information on the reactivity of **1** with halogenated hydrocarbons and to try to freeze out the intramolecular hydrogen exchange in **1**, we decided to prepare cold solutions of **1** in a mixture of deuterated Freons. **1** was not soluble in Freons in the absence of $CDCl_3$. The reactions were therefore carried out in the solvent mixture ($CDCl_3$:$CDFCl_2$:$CDF_2Cl$ = 1:5:5) described in the Experimental Section. This mixture allows liquid-state NMR measurements down to 140 K.[17] Figure 4 shows the 500 MHz NMR spectra of a sample measured after storage at 240 K for several days. At 263 K, the highest accessible temperature in this medium, three main signals **a/b**, **f**, and **e** are observed in the high-field spectrum characterized by different spectral changes upon lowering the temperature. The triplet **e** appearing at −8.9 ppm corresponds to the starting complex **1**. The signal broadens near 143 K but does not split into separate signals for dihydrogen and hydride sites, which demonstrates the fast intramolecular hydride−dihydrogen exchange within this species. The line broadening at low temperatures could arise either from the circumstance that this exchange becomes slower or from a short $T_2$ arising from the increase in viscosity of the solution or rapid dipole−dipole relaxation. Signal **f** appears at −15.1 ppm and consists of a triplet with $J^{av}_{PH} = 11$ Hz. It broadens slightly when the temperature is lowered, and its intensity increases with the sample storage time. It was assigned to a species (**2′**) similar to $RuHCl(H_2)(PCy_3)_2$ (**2**), a complex previously obtained from the reaction of **1** with $CH_2Cl_2$, but not to **2** itself, which resonates at −16.8 ppm and exchanges in the presence of excess dihydrogen with $RuHCl(H_2)_2(PCy_3)_2$ (**3**), also present as discussed below.[12b] Peak **g**, appearing at 5.3 ppm, was assigned to $CDHCl_2$ formed during the reaction together with **2′** and **3**.

(15) Bée, M. *Quasielastic Neutron Scattering*; Adam Hilger: Bristol, U.K., 1988.
(16) Hewson, A. C. *J. Phys. C: Solid State Phys.* **1982**, *15*, 3855.
(17) Siegel, J. S.; Anet, F. A. L. *J. Org. Chem.* **1988**, *53*, 2629.

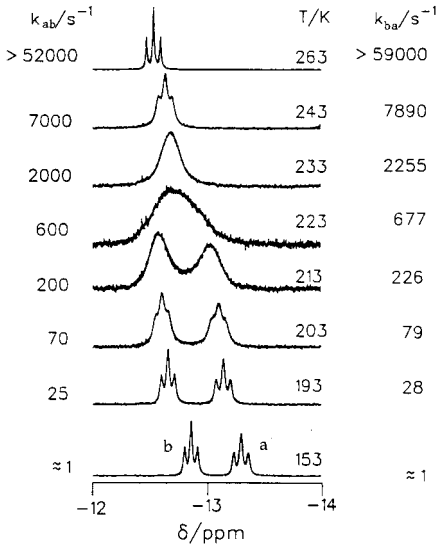


**Figure 5.** Superposed experimental and calculated NMR signals **a** and **b** of the spectra shown in Figure 4.

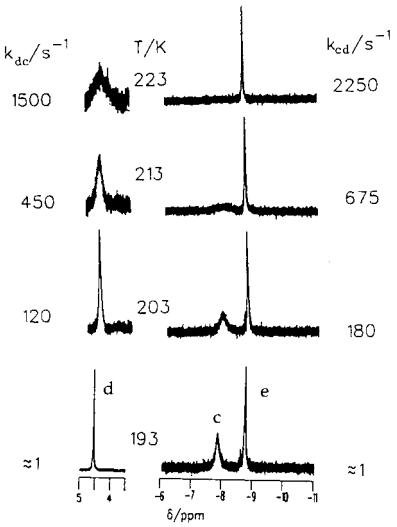


**Figure 6.** Superposed experimental and calculated NMR signals **c** and **d** of the spectra shown in Figure 4.

The major signal is a triplet labeled **a/b**, appearing at −12.6 ppm ($J_{PH}$ = 31 Hz), and was assigned to the new complex $RuH_2Cl_2(PCy_3)_2$ (**4**), the synthesis and characterization of which will be described in section 5.

The spectra exhibited interesting changes when the sample was cooled. First, the signal due to **4** broadened and then split into two sharp triplets labeled as **a** and **b** in Figure 5, at −12.7 ppm ($J_{PH}$ = 29 Hz) and −13.2 ppm ($J_{PH}$ = 32 Hz). The coalescence temperature is 220 K. The intensity ratio $I_a/I_b$ of these peaks was found to be 1.13. Therefore, the line broadening of signal **b** is more pronounced than that of signal **a** when temperature is increased, and the line shape is strongly asymmetric at the coalescence point (∼220 K). The longitudinal relaxation times $T_1$ were measured at 183 K and 500 MHz. We obtained a common value of 430 ms for each triplet in agreement with a classical dihydride formulation.

In addition to signals **a** and **b**, two new broad peaks appeared at −7.9 (signal **c**) and 4.6 ppm (signal **d**; see Figures 4 and 6). Signal **c** was assigned by comparison to a preceding experiment with $RuH(H_2)_2I(PCy_3)_2$[12b] to $RuH(H_2)_2Cl(PCy_3)_2$ (**3**), for which a $T_1$ value of 22 ms was measured at 183 K (500 MHz). Signal **d** corresponds to free dihydrogen and sharpens when the temperature is lowered. Exchange between free and coordinated $H_2$ explains the line broadening of both signals when the temperature is increased. Unfortunately, it was not possible to heat the samples in order to reach the fast exchange regime exhibiting one coalesced line. As in the case of **1**, only one signal is observed for the metal-bound hydrogen atoms of **3**, indicating a fast intramolecular hydrogen−dihydrogen conversion. Line broadening of signal **c** occurs at very low temperatures for the same reasons as discussed in the case of **1**. In this Freon mixture, in the presence of excess $H_2$ (released from reaction), we observe not the 16-electron complex **2** but the 18-electron species **3**. In preceding experiments carried out in toluene-$d_8$, we could see both the 16-electron $RuH(H_2)I(PCy_3)_2$ and the 18-electron $RuH(H_2)_2I(PCy_3)_2$, even under 6 bar of dihydrogen.[12b] In the present case, the exclusive observation of **3** could result from a better solubility of dihydrogen in Freons.

**Scheme 1**

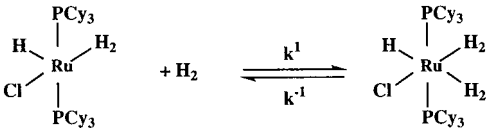


**2** **3**

**Scheme 2**

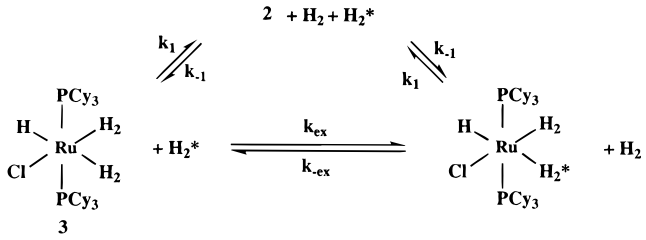


A line shape analysis of signals **a**−**d** was carried out in order to obtain quantitative kinetic parameters. The superposed experimental and calculated spectra are shown in Figures 5 and 6. The line shape simulations of signals **a** and **b** were based on usual two-state exchange between two unequally populated environments **a** and **b**, corresponding to signals **a** and **b**. The mole fraction $x_a = 1 - x_b = 0.47$ was obtained by line shape analysis in the slow exchange region and found to be independent of temperature within the margin of error. The chemical shifts $\delta_a$ and $\delta_b$ were slightly temperature dependent and were extrapolated to high temperature. The agreement between the experimental and calculated spectra is excellent, as indicated in Figure 5. The rate constants obtained can be expressed as

$$k_{ab} = 10^{14}\exp(-47\ \text{kJ mol}^{-1}/RT), \quad 193 < T < 243\ \text{K}, \qquad k_{ab}(223\ \text{K}) = 600\ \text{s}^{-1} \quad (1)$$

In principle, the line shape of signals **c** and **d** in Figure 6 could be described in terms of Scheme 1, which corresponds to exchange between free and coordinated $H_2$. However, in the case of the spectra of Figure 6, the concentration of **2** is too small to be detected and does not influence the actual line shape any more. According to arguments described previously,[18] the line shape equation can then no longer be based on Scheme 1 but must be based on Scheme 2 where **2** is a nonobserved intermediate. Scheme 2 can be abbreviated by the equation

(18) Limbach H. H. *J. Magn. Reson.* **1979**, *36*, 287.

$$H_2(\text{free}) + H^*_2(3) \overset{k_{ex}}{\rightleftharpoons} H^*_2(\text{free}) + H_2(3) \qquad (2)$$

where $H_2$(free) (signal **d**) corresponds to free dissolved dihydrogen and $H_2(3)$ to dihydrogen bound to Ru in **3** (signal **c**). Some uncertainty is introduced because of the short $T_2$ of **3** at low temperatures. The quantities obtained by line shape simulations are $k_{dc}$ and $k_{cd}$, where

$$k_{cd} = v/c\{H_2(3)\} = k_{ex}\, c\{H_2(\text{free})\}$$

$$k_{dc} = k_{cd}\, x_d/x_c = v/c\{H_2(\text{free})\} = k_{ex}\, c\{H_2(3)\} \qquad (3)$$

$k_{ex}$ is the pseudo-second-order rate constant of the reaction and $v$ its velocity. $c\{i\}$ represent the concentrations and $x_i$ the mole fractions. A formal kinetic analysis of the reaction network of Scheme 2 using the usual steady-state condition for the intermediate **2** shows that $k_{ex}$ is related to $k_1$ and $k_{-1}$ as follows:

$$k_{ex} = (k_1 k_{-1})/(k_{-1} + k_{-1}) = k_1/2 \qquad (4)$$

The $c\{i\}$ were not exactly known but were estimated to be less than 0.1 mol $L^{-1}$. By contrast, the mole fractions $x_c = 1 - x_d = c\{H_2(3)\}/(c\{H_2(\text{free})\} + c\{H_2(3)\}) = 1 - x_d$ were obtained by line shape analysis and found to be independent of temperature; i.e., $x_c = 1 - x_d = 0.6$. Finally, we obtained

$$k_{ex}\, c\{H_2(\text{free})\} = 1.5 k_{ex}\, c\{H_2(3)\} = 10^{14} \exp(-47 \text{ kJ mol}^{-1}/RT),\ 203 < T < 223 \text{ K}$$

$$k_{ex}\, c\{H_2(\text{free})\}(223 \text{ K}) = 1500 \text{ s}^{-1}$$

Since $c\{H_2(\text{free})\} < 0.1$ mol $L^{-1}$, it follows that the preexponential factor characterizing the exchange is larger than $10^{14}$ $s^{-1}$. However, because of the limited range where rate constants could be obtained, all kinetic parameters are only rough estimates.

## 4. Theoretical Study of a Model for 1

**(i) Stability of Different Isomers.** Several different isomers may be envisaged for **1**, depending on the relative orientations of the various ligands. As the $PCy_3$ ligands involved in **1** itself contain too many atoms for a reliable ab initio study with current technology, we replaced them by $PH_3$. This is a standard approximation, which should not significantly affect the results obtained. The most important isomers of **1** are sketched in Figure 7, which shows the atom-labeling scheme used. All may be described as essentially octahedral with two trans phosphines; the steric bulk of the $PCy_3$ ligands in the real complex **1** ensures that they cannot occupy cis positions.

Isomer **1a** has $C_{2v}$ symmetry. All six hydrogen atoms coordinated to Ru lie in a plane which contains the $C_2$ axis, and the two hydride ligands are cis. In the case of isomer **1b**, which also has $C_{2v}$ symmetry, the two $H_2$ ligands are perpendicular to the plane which contains the $C_2$ axis. A lower symmetry ($C_s$) defines **1c**, in which the mirror plane contains the two hydrides and just one of the dihydrogen ligands, the other $H_2$ unit being perpendicular to that plane. All the six hydrogen atoms coordinated to Ru again lie in a plane for isomer **1d** ($C_{2h}$), but the two hydrides are now trans.

These four isomers, together with several others of lesser importance,[19] were investigated theoretically using Hartree−Fock (HF), second-order Möller−Plesset perturbation theory (MP2), and density functional methods. A hybrid form of density functional theory (DFT) usually known as B3LYP was adopted.[20] This method has already been shown to be appropriate for the study of the electronic structures and properties of dihydrogen complexes.[21−23] It is now widely agreed that the MP2 method is less reliable for transition-metal complexes than

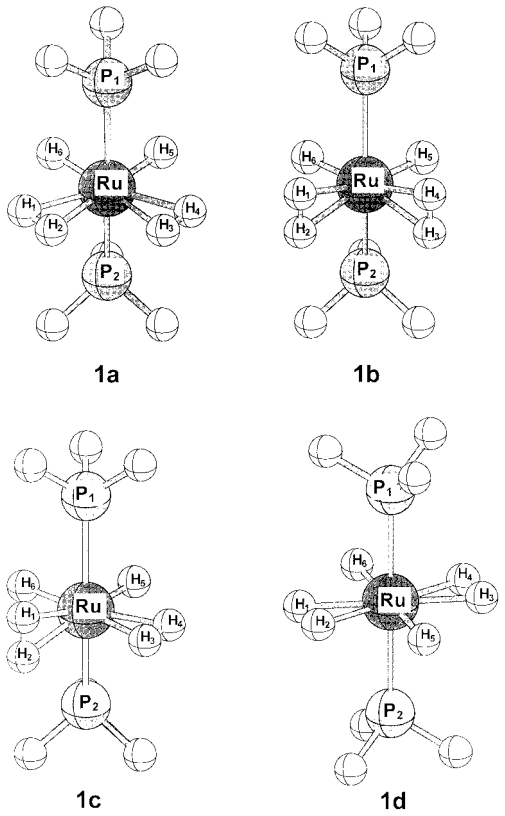


**Figure 7.** The four isomeric structures of **1**, $RuH_2(H_2)_2(PH_3)_2$, considered in this work.

**Table 1.** Selected Geometrical Parameters (Å and deg) of the DFT/B3LYP Optimized Stationary Points in the $RuH_2(H_2)_2(PH_3)_2$ Model Complex (Basis Set B)

| | **1a** ($C_{2v}$) | **1b** ($C_{2v}$) | **1c** ($C_s$) | **1d** ($C_{2h}$) |
|---|---|---|---|---|
| Ru−H1 | 1.784 | 1.809 | 1.805 | 1.709 |
| Ru−H2 | 1.818 | 1.809 | 1.805 | 1.709 |
| Ru−H3 | 1.818 | 1.809 | 1.808 | 1.709 |
| Ru−H4 | 1.784 | 1.809 | 1.776 | 1.709 |
| Ru−H5 | 1.621 | 1.621 | 1.619 | 1.682 |
| Ru−H6 | 1.621 | 1.621 | 1.624 | 1.682 |
| Ru−P1 | 2.311 | 2.306 | 2.310 | 2.323 |
| Ru−P2 | 2.311 | 2.306 | 2.310 | 2.323 |
| H1−H2 | 0.853 | 0.846 | 0.846 | 0.913 |
| H3−H4 | 0.853 | 0.846 | 0.858 | 0.913 |
| P1−Ru−P2 | 163.8 | 151.0 | 158.6 | 180.0 |
| H1−Ru−H2 | 27.4 | 25.1 | 27.1 | 31.0 |
| H2−Ru−H3 | 72.9 | 91.2 | 84.0 | 149.0 |
| H3−Ru−H4 | 27.4 | 25.1 | 27.7 | 31.0 |
| H4−Ru−H5 | 75.8 | 89.7 | 77.2 | 105.5 |
| H5−Ru−H6 | 80.7 | 89.4 | 83.6 | 180.0 |
| H6−Ru−H1 | 75.8 | 89.7 | 87.8 | 74.5 |

(19) Barthelat, J.-C.; Hussein, K.; Marsden, C. J. Manuscript in preparation.

(20) (a) Becke, A. D. *J. Chem. Phys*. **1993**, *98*, 1372 and 5648. (b) Lee, C.; Yang, W.; Parr, R. G. *Phys. Rev. B* **1988**, *37*, 785.
(21) (a) Gelabert, R.; Moreno, M.; Lluch, J. M.; Lledos, A. *Organometallics* **1997**, *16*, 3805. (b) Ricca, A.; Bauschlicher, C. W. *Chem. Phys. Lett.* **1995**, *245*, 150. (c) Siegbahn, P. E. M. *J. Am. Chem. Soc*. **1996**, *118*, 1487.
(22) Bernardi, F.; Bottoni, A.; Calcinari, M.; Rossi, I.; Robb, M. A. *J. Phys. Chem. A* **1997**, *101*, 6310.
(23) Bytheway, I.; Backsay, G. B.; Hush, N. S. *J. Phys. Chem*. **1996**, *100*, 6023.

**Table 2.** Relative Energies (kcal/mol) of the Optimized Stationary Points in the $RuH_2(H_2)_2(PH_3)_2$ Model Complex

| | HF//HF | | MP2//MP2 | | DFT//DFT | | | MP2//DFT/B | MP4SDQ//DFT/B | CCSD(T)//DFT/B |
|---|---|---|---|---|---|---|---|---|---|---|
| basis set | A | B | A | B | A | B | C | C | C | C |
| **1a** | 0.0 | 0.0 | 0.45 | 0.0 | 0.0 | 0.0 | 0.0 | 0.02 | 0.0 | 0.0 |
| **1b** | 0.69 | 1.29 | 1.77 | 1.15 | 1.63 | 1.99 | 1.97 | 1.22 | 1.79 | 1.43 |
| **1c** | 0.73 | 1.07 | 0. | | 0.82 | 0.99 | 0.95 | 0. | 0.13 | 0.26 |
| **1d** | 6.52 | 5.32 | 15.33 | 12.59 | 11.64 | 10.51 | | | | |

is DFT; our present results, discussed below, provide further support for this assertion.

Geometrical parameters optimized for the four isomers **1a**−**d** at the B3LYP/basis B level of theory are presented in Table 1. The most interesting structural aspect of these complexes is probably the length of the H−H bond in the coordinated dihydrogen ligand, relative to its value in free $H_2$. We find an increase in bond length of 12.4% for isomer **1a** at the B3LYP level of theory, with very similar changes for **1b** and for **1c**. MP2 theory predicts a greater lengthening of the H−H bond, by about 20%. It has already been noted that MP2 theory overemphasizes donation into the $\sigma^*$ H−H antibonding orbital, compared to DFT methods;[23] the comparison of DFT, MP2, and CCSD(T) relative energies presented below for isomers of **1** leads us to consider the DFT results as more reliable for these nonclassical complexes.

Relative energies for the different isomers obtained at various levels of theory with bases A, B, and C are reported in Table 2. It is clear that the three isomers **1a**−**c**, which differ only in the orientations of the dihydrogen ligands relative to the plane containing Ru and the two hydrides, are very close in energy (separations of the order of 1−2 kcal/mol), whereas isomer **1d**, in which the two hydride ligands are trans, is substantially less stable (by some 10−15 kcal/mol) than the others. Isomer **1a** is consistently the most stable using HF, DFT, or CCSD(T) methods, irrespective of the basis used. However, the results obtained with MP2 theory are inconsistent; basis A gives a small preference for **1c** over **1a**, whereas isomer **1c** is no longer a stationary point on the potential surface with the more complete basis B, as the $H_2$ unit in the plane splits to give two hydride ligands, increasing the oxidation state of Ru to IV. If there is an inconsistency between CCSD(T) and MP2 results, we clearly prefer the far more rigorous CCSD(T) values, and since the DFT and CCSD(T) results for the energy separations between isomers are fairly similar, we believe that the DFT results should be preferred over MP2 data. Other authors previously noted that DFT theory gives results in good agreement with more elaborate (CASPT2) methods for organometallic complexes. Even though the energetic preference for a coplanar arrangement of all six H atoms bound to Ru in **1** is slight, we believe it to be real; the consistency of the HF, DFT, and very high-level CCSD(T) results is striking.

The nature of each of these four stationary points on the potential energy surface was determined by calculation of the vibrational frequencies, using basis A. The two isomers **1a** and **1b** are found to be true minima, whatever level of theory is used. Isomer **1c** has one imaginary vibrational frequency at the HF and DFT levels. However, it is a minimum at the MP2 level. Isomer **1d** is a true minimum only at the HF level. The relatively high energy calculated for isomer **1d** is consistent with the IR spectrum of **1**, which was interpreted to indicate a *cis*-dihydride geometry. Before analyzing the cis−trans issue, we consider the preference for coplanarity of the six H atoms bound to Ru.

The electronic origins of this preference may be traced to the interaction which has been named the "cis effect". The

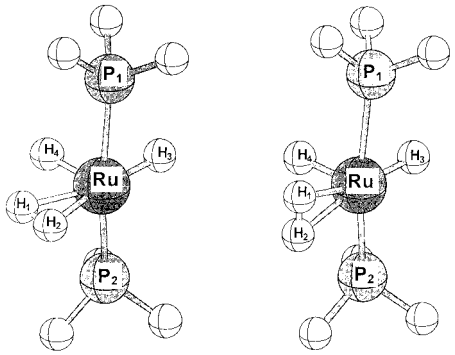


**5a** **5b**

**Figure 8.** Two isomeric structures of $RuH_2(H_2)(PH_3)_2$.

**Table 3.** Relative Energies (kcal/mol) and Selected Geometrical Parameters (Å and deg) of DFT/B3LYP Optimized Stationary Points in the $RuH_2(H_2)_2(PH_3)_2$ Model Complex (Basis Set B)

| | **5a** ($C_s$) | **5b** ($C_s$) |
|---|---|---|
| Ru−H1 | 1.767 | 1.804 |
| Ru−H2 | 1.800 | 1.804 |
| Ru−H5 | 1.635 | 1.563 |
| Ru−H6 | 1.565 | 1.630 |
| Ru−P1 | 2.303 | 2.300 |
| Ru−P2 | 2.303 | 2.300 |
| H1−H2 | 0.860 | 0.850 |
| P1−Ru−P2 | 164.9 | 157.9 |
| H1−Ru−H2 | 27.9 | 27.2 |
| H2−Ru−H5 | 170.3 | 166.4 |
| H5−Ru−H6 | 87.0 | 89.2 |
| H6−Ru−H1 | 74.8 | 90.2 |
| $\Delta E$ | 0.0 | 0.79 |

effect has been discussed by Eisenstein and co-workers in connection with molecule **2**, $RuH(H_2)I(PCy_3)_2$.[12,24] The Ru−H $\sigma$ bonding orbital can be partly delocalized into the $\sigma^*$ H−H antibonding orbital of a neighboring $H_2$ ligand, providing that all four atoms are coplanar. The effect will clearly be maximized in **1a**, in which all six H atoms are coplanar, absent in **1b** where symmetry prevents its operation, and partly present in **1c**. Wishing to discover whether this stabilizing cis effect may be used to rationalize the structural preferences of dihydrogen complexes in general, rather than being limited just to complex **1**, we have also investigated two related systems, $RuH_2(H_2)(PH_3)_2$ (**5**), sketched in Figure 8, and $RuHCl(H_2)_2(PH_3)_2$ (**3**).

We have undertaken B3LYP geometry optimizations (basis B) of isomers **5a** and **5b**, which differ only by the orientation of the dihydrogen ligand with respect to the plane containing Ru and the two hydrides. Structural parameters are reported in Table 3. **5a**, in which the cis effect can operate because the $H_2$ unit is coplanar with the hydrides, is slightly more stable than **5b**, by just 0.8 kcal/mol. The geometries of the four isomers **3a**−**d** have been optimized at the same level of theory.

(24) Van der Sluys, L. S.; Eckert, J.; Eisenstein, O.; Hall, J. H.; Huffman, J. C.; Jackson, S. A.; Koetzle, T. F.; Kubas, G. J.; Vergamini, P. J.; Caulton, K. G. *J. Am. Chem. Soc.* **1990**, *112*, 4831.

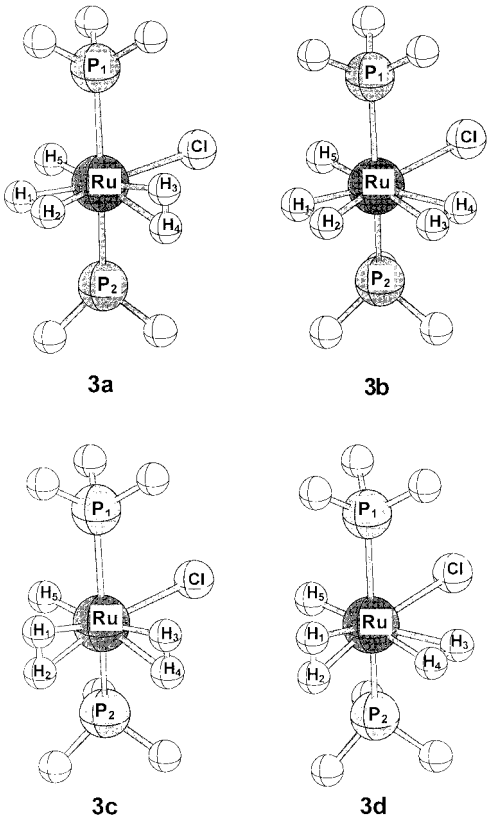


**Figure 9.** The four isomeric structures of $RuHCl(H_2)_2(PH_3)_2$ (**3**).

They are sketched in Figure 9. If the cis effect operates for the Ru−H bond, the dihydrogen close to the hydride will lie in the equatorial plane. Since Cl is more electronegative than H, one does not anticipate that there will be a significant tendency of the Ru−Cl bonding orbital to delocalize. In the absence of any cis effect involving the Ru−Cl bond, the $H_2$ unit adjacent to Cl may be expected to lie perpendicular to the other $H_2$, to allow maximal interaction with the Ru d orbitals; if the two dihydrogens are coplanar, they are effectively competing for the same d orbitals on Ru. We note that the two $H_2$ units in $Co(H_2)_2^+$ are indeed perpendicular,[25] as are the two ethylene ligands in $Ni(C_2H_4)_2$.[22]

The lowest-energy isomer of **3** is **3a**, which follows exactly the predictions based on the cis effect. It has $C_s$ symmetry and is a minimum on the potential energy surface. Isomers **3b** and **3c** both contradict the predictions of the cis effect rule, in one respect, because the $H_2$ unit cis to Cl lies in the plane for **3b**, whereas the $H_2$ cis to H is perpendicular to the plane for **3c**. One imaginary vibrational frequency is found for both isomers, and in each case, that motion corresponds to the $H_2$ rotation which leads to isomer **3a**. The relative energies of these isomers are given in Table 4; the differences are small, as are those of the isomers **1a**−**c**. We note that the orientational preference (rotation barrier) is nearly twice as great for the $H_2$ adjacent to H (isomer **3c**) as for that adjacent to Cl (isomer 3**b**), showing the importance of the cis effect. The least stable isomer is **3d**, for which both $H_2$ orientations contradict the cis effect rule; two imaginary vibrational frequencies are found for this isomer, corresponding to the two $H_2$ rotations needed to return to isomer **3a**. While we do not wish to overinterpret rather small energy differences, we note that the energy separation between **3a** and **3d** is close to that obtained simply by adding the relative energies of **3b** and **3c**, suggesting a weak coupling between the rotational motions of the two $H_2$ ligands. This comparison of three different systems reveals a consistent picture; the most stable isomer in each case is that which would be predicted by the cis effect, an effect already analyzed in the literature.

**Table 4.** Relative Energies (kcal/mol) and Selected Geometrical Parameters (Å and deg) of DFT/B3LYP Optimized Stationary Points in the $RuHCl(H_2)_2(PH_3)_2$ Model Complex (Basis Set B)

| | **3a** ($C_s$) | **3b** ($C_s$) | **3c** ($C_s$) | **3d** ($C_s$) |
|---|---|---|---|---|
| Ru−H1 | 1.658 | 1.633 | 1.699 | 1.695 |
| Ru−H2 | 1.681 | 1.691 | 1.699 | 1.695 |
| Ru−H3 | 1.868 | 1.923 | 1.865 | 1.892 |
| Ru−H4 | 1.868 | 1.913 | 1.865 | 1.881 |
| Ru−H5 | 1.597 | 1.591 | 1.600 | 1.596 |
| Ru−Cl | 2.463 | 2.465 | 2.461 | 2.468 |
| Ru−P1 | 2.339 | 2.337 | 2.340 | 2.341 |
| Ru−P2 | 2.339 | 2.337 | 2.340 | 2.341 |
| H1−H2 | 0.945 | 0.938 | 0.899 | 0.904 |
| H3−H4 | 0.820 | 0.802 | 0.821 | 0.810 |
| P1−Ru−P2 | 162.9 | 166.5 | 156.7 | 161.4 |
| H1−Ru−H2 | 32.9 | 32.5 | 30.7 | 30.9 |
| H2−Ru−H3 | 81.9 | 70.5 | 95.6 | 83.2 |
| H3−Ru−H4 | 25.4 | 24.1 | 24.5 | 24.8 |
| H4−Ru−Cl | 86.3 | 71.7 | 88.5 | 76.7 |
| Cl−Ru−H5 | 87.3 | 87. | 91.1 | 88.9 |
| H5−Ru−H1 | 71.9 | 71.1 | 88.1 | 86.7 |
| $\Delta E$ | 0.0 | 1.33 | 2.25 | 3.13 |

The low stability of **1d** compared to **1a** could be anticipated, given the generally accepted high "trans influence" of the hydride ligand. From an orbital point of view, we find that the preference for a cis orientation of the two hydrides in **1** may be traced to the nature of the two MOs which are primarily responsible for Ru−H bonding. Bonding between Ru and dihydrogen does not give rise to any particular preferred orientation of these ligands. Both Ru−H bonding MOs involve Ru d orbitals for **1a**, but only one MO with good Ru−H bonding overlap can be constructed using Ru d orbitals if the two hydrides are trans, the other MO involving a 5p orbital on Ru which is at substantially higher energy than the 4d set. As a consequence of these orbital differences, we note that the Ru−hydride bond lengths in **1a** are substantially shorter than the distances between Ru and the H atoms of the dihydrogen ligands, by 0.18 Å on average, whereas in **1d**, with weak Ru−H bonds, the difference is only 0.027 Å.

The IR spectrum of **1** provides valuable information on the nature and strength of the Ru−H and Ru−($H_2$) interactions; as the spectrum has been recorded and partially assigned,[6a] a comparison with the calculated values provides a stringent test of the quality of the computed data. Two very intense bands are seen at 1927 and 1890 $cm^{-1}$, assigned to Ru−H stretching motions; however, no absorption was observed which could be attributed to stretching either of the $H_2$ units or of the Ru−($H_2$) bonds. The calculated harmonic wavenumbers (B3LYP/basis B) for the two Ru−H stretching vibrations in **1a** are 2031 ($a_1$) and 1995 ($b_2$) $cm^{-1}$; both modes are indeed intense, with absolute intensities of 112 and 134 km/mol, respectively. While the calculated harmonic frequencies are therefore some 5.5% higher than the observed fundamentals, a typical margin of error,[26] we note that the difference in frequency between the two modes is very well reproduced. The stretching motions of the two $H_2$ units are predicted at 3038 ($a_1$) and 3017 ($b_2$) $cm^{-1}$, with high absolute intensities of 112 and 140 km/mol, respectively. This result is surprising, given the known low intensity of H−H stretches which have been detected,[1,7] and one might

(25) Bauschlicher, C. W.; Maitre, P. *J. Phys. Chem.* **1995**, *99*, 3444.

(26) Wong, M. W. *Chem. Phys. Lett.* **1996**, *256*, 391.

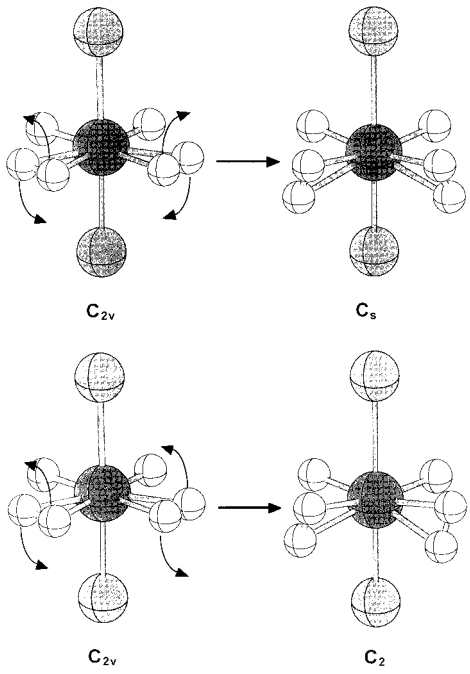


**Figure 10.** The two possible pathways for rotation of the two dihydrogen ligands in **1**. Hydrogen atoms of the $PH_3$ groups have been omitted for clarity.

suppose that such intense bands would be readily detectable; unfortunately, they are likely to be masked in the real system by the many C−H stretching modes within the $PCy_3$ ligands. Two twisting motions of the $H_2$ units in the $RuH_2(H_2)_2$ plane are predicted at 1640 and 1635 $cm^{-1}$, with moderate to low intensity (44 and 4 km/mol, respectively), while the vibrations best described as Ru−($H_2$) stretches are predicted at 997 ($a_1$) and 925 ($b_2$) $cm^{-1}$, but these are both weak with intensities of only 2 and 7 km/mol. The vibrational wavenumbers were also obtained for **1a** at the MP2 level of theory using basis A. For the two Ru−H stretching motions, the values are 2123 ($a_1$) and 2116 ($b_2$) $cm^{-1}$; these are substantially poorer than those obtained using DFT methods, both for the absolute values of the wavenumbers, in error here by some 10−11%, and for the separation between the two modes (only 7 $cm^{-1}$, compared to 37 $cm^{-1}$ experimentally or 34 $cm^{-1}$ with B3LYP theory). These results provide another indication that the B3LYP method is more successful than low-order perturbation theory for the study of organometallic complexes. It is encouraging to note that extension of the basis from A to B changes the B3LYP wavenumbers for these two modes by no more than 4 $cm^{-1}$.

**(ii) Rotation of Dihydrogen Ligands in 1.** Since the INS spectra described above (section 2) have shown that rotation of the dihydrogen ligands in **1** is facile, there is an obvious interest in a theoretical study of the potential function for $H_2$ rotation in **1**. As there are two equivalent dihydrogen ligands, both must participate in the process detected by INS, but it is not clear a priori whether the two ligands rotate in the same or in opposite directions or, indeed, whether the coupling between the motion of the two $H_2$ units is sufficiently strong for a perceptible difference to exist between the two possibilities. The two possible pathways from **1a** to **1b** are sketched in Figure 10; if the two ligands rotate in opposite senses, a $C_s$ surface is followed, whereas rotation of the two $H_2$ units in the same senses generates a $C_2$ pathway. Our most important findings are displayed in Figure 11, which shows that the calculated rotation barriers are very small.

We initially scanned the whole of both the $C_2$ and $C_s$ surfaces,

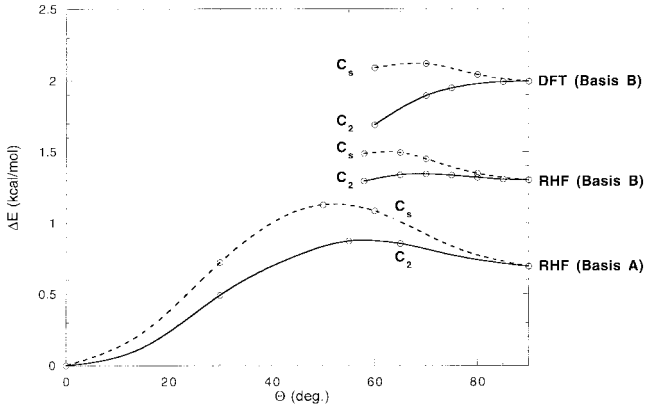


**Figure 11.** RHF and DFT energy profiles for rotation of the two $H_2$ ligands in $RuH_2(H_2)_2(PH_3)_2$. Θ indicates the dihedral angle between the Ru($H_2$) and Ru($H)_2$ planes.

at the RHF level of theory using basis A. While the results obtained at this level may not be quantitatively reliable, the qualitative features should be informative. Fixed angles of rotation of the $H_2$ units were adopted, with respect to the plane containing the Ru and the two hydride ligands, and the remaining independent geometrical parameters (19 for the $C_2$ pathway, 21 for the $C_s$) were optimized. It may be seen from Figure 11 that the $C_2$ pathway is consistently preferred over the $C_s$ and that the maximum along the pathway is closer to **1b**, consistent with the greater stability of **1a** than of **1b**. In view of the substantial computational effort needed to scan the entire $C_2$ and $C_s$ surfaces at higher levels of theory, we concentrated our attention on those parts of the surfaces near the higher-energy isomer **1b**, i.e. Θ angles near 90°. Extension of the basis from A to B increases the RHF barrier to $H_2$ rotation somewhat, from 0.9 to 1.3 kcal/mol, and moves the transition state closer to **1b**; that isomer remains a true minimum, though the magnitude of its lowest vibrational frequency drops sharply. When electron correlation effects are included at the B3LYP level of theory with basis B, the barrier increases again, from 1.3 to 2.0 kcal/mol; more importantly, **1b** now becomes a transition state, as it is a local maximum on the $C_2$ surface. Thus as the level of theory adopted is improved, the derived potential governing $H_2$ rotation becomes progressively closer to the simple 2-fold cosine function used in analysis of the INS data. In particular, we may take the energy difference between **1a** and **1b** to represent the potential barrier. Our B3LYP/basis B value of 2.0 kcal/mol for this barrier agrees remarkably well with the result inferred from the INS data (2.2 kcal/mol, assuming uncoupled rotation of the two $H_2$ molecules). However, the presumably more reliable CCSD(T) value for the barrier obtained with basis C is a little smaller, at 1.4 kcal/mol, so the particularly good agreement at the DFT/basis B level is probably fortuitous. The qualitatively important point is that the calculated barrier height agrees rather well with that derived from experiment with the use of a simplified model. We may also note that the barrier to rotation along the $C_s$ pathway is only slightly higher, by some 0.1 kcal/mol, than that for coupled $C_2$ rotation, so at most temperatures both pathways will in fact be followed. The effects of basis extension on the calculated barrier are not large; we note in particular that the DFT result with basis C differs from that with basis B by an utterly trivial amount (0.02 kcal/mol). This agreement for the barrier therefore suggests that the other calculated results are also reliable.

### 5. NMR Studies of 1 in $CDCl_3$: Synthesis and Theoretical Studies of $RuH_2Cl_2(PCy_3)_2$ (4)

**(i) Synthesis and NMR Studies.** Since we suspected that **4** resulted from the reaction of **1** with the chloroform present in Freon, the direct reaction of **1** with $CDCl_3$ was carried out in an NMR tube. Vigorous $H_2$ evolution was immediately observed, and only one triplet signal at $-12.38$ ppm ($J_{P-H}$ = 31.5 Hz) was detected in the high-field region which corresponded to **4**. When the sample was cooled to 233 K, the signal broadened and split into two broad triplets, well resolved in Freon (vide supra) or in a mixture of $CDCl_3/CD_2Cl_2$ at 183 K. The $^{31}P\{^1H\}$ NMR spectrum in $CDCl_3$ at 297 K presents a singlet at 91.3 ppm split into a triplet with $J_{P-H}$ = 31.7 Hz after decoupling of the protons of the cyclohexyl groups. This is demonstrative of the presence of two hydrides bound to the ruthenium. At 208 K, the $^{31}P\{^1H\}$ NMR spectrum in $CDCl_3$ consists of two broad singlets at 97.1 and 83.1 ppm (integration ratio 1.1:1) in agreement with the observations recorded in $^1H$ NMR. Interestingly, the appearance of **4** is not accompanied by the formation of $CDHCl_2$ as monitored by $^1H$ NMR. However, as the signal characteristic for **4** disappears, a new signal appears at $+5.28$ ppm (1:1:1 triplet, $J_{H-D}$ = 0.9 Hz) attributed to $CDHCl_2$ formed during the decomposition. The chloride ruthenium compounds then formed were not characterized.

Attempts at isolating **4** by reacting **1** with $CHCl_3$ using different experimental procedures (2-fold or excess $CHCl_3$ in pentane or THF, pure $CHCl_3$) failed because of the lack of stability of **4** in the presence of $CHCl_3$. For example, the beige solid obtained from pure chloroform after evaporation and washing in pentane is a mixture of unidentified chloride ruthenium complexes and the dihydride complex **4**. Similar results were obtained when **1** was reacted with $CCl_4$, $Cl_2$, or HCl (either gas or aqueous solution) in THF. Nevertheless, addition of aqueous HCl to a suspension of **1** in $Et_2O$ yielded a pink suspension which after filtration and washing with pentane was identified by $^1H$ and $^{31}P$ NMR as pure **4** (yield 60%). All data were then consistent with the formulation $RuH_2Cl_2(PCy_3)_2$. **4** is therefore a 16 electron complex and a rare example of a ruthenium(IV) polyhydride. During the preparation of this paper, Werner et al. reported the preparation of the very similar complex $RuH_2Cl_2(P^iPr_3)_2$ (**4-*i*Pr**) identified by an X-ray crystal structure.[13] Several ruthenium(IV) hydrido derivatives have been described,[27−29] and we reported a few years ago the synthesis of a similar but 18-electron complex $RuH_2(OCOCF_3)_2(PCy_3)_2$. Interestingly, the latter compound, although electronically saturated, was shown to be thermally unstable and to lose $H_2$ slowly in solution. A similar pathway is probably responsible for the degradation of **4** in solution. **4** is also analogous to the osmium derivative $OsH_2Cl_2(PCy_3)_2$ (**4-Os**), prepared and studied by Berke and Caulton.[31] The spectroscopic properties of both compounds are very similar, but as expected, the osmium complex is more stable. A fluxional process is present in both compounds, and a decoalescence into two sets of signals corresponding to two interconverting isomers is apparent at low temperature. That the different signals observed for **4** below 203 K correspond to two isomers rather than to one asymmetric complex results from the integration ratio in $^{31}P$ and $^1H$ NMR which give reproducibly a 1.1:1 ratio and from asymmetry in the coalescence spectrum as evidenced by line shape analysis (vide supra). However, although **4-Os** is shown to consist of a mixture of a symmetric (minor) and an asymmetric (major) complex, the structures of which have been proposed after ab initio calculations, complex **4** exists as two symmetric interconverting isomers. It is not possible to rule out the possibility for each triplet to result from the presence of fast interconverting asymmetric isomers even at very low temperature in Freons. This would however contradict the results of the theoretical calculations (vide infra).

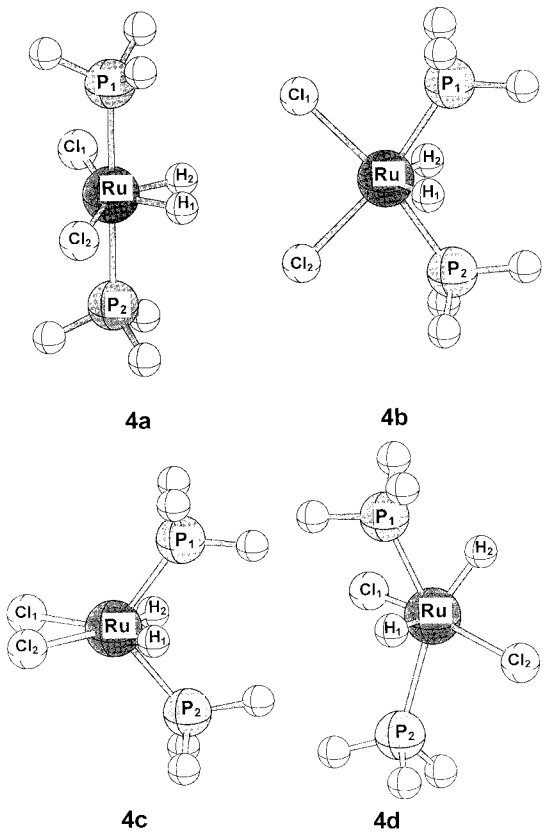


**Figure 12.** Isomeric structures of **4**, $RuH_2Cl_2(PH_3)_2$.

**4** does not react with $H_2$ in benzene but does react with CO to give $RuHCl(CO)_2(PCy_3)_2$, identified by comparison with an authentic sample.[12b] The reaction proceeds through selective reductive elimination of HCl rather than that of $H_2$ or $Cl_2$ which is rather surprising.

**(ii) Theoretical Study of a Model for 4.** To make feasible a computational study of the structures and energies of possible isomers of **4**, we adopted the "standard" approximation of replacing the $PCy_3$ phosphines by $PH_3$, to give **4**, whose formula is thus $RuH_2Cl_2(PH_3)_2$. Geometries were optimized using B3LYP theory and basis B. Several isomers were studied, of which the four most important are sketched in Figure 12, which also indicates the atomic numbering scheme. Optimized structural parameters and relative energies are reported in Table 5.

Although the coordination about Ru in **4** might be regarded as octahedral, there are substantial deviations from the idealized values of 90 or 180° for some bond angles in each of **4a**−**d**, so much so that the octahedral paradigm is misleading. Isomer

(27) (a) Baird, G. J.; Davies, S. G.; Moon, S. D.; Simpson, S. J.; Jones, R. H. *J. Chem. Soc., Dalton Trans.* **1985**, 1479. (b) Arliguie, T.; Border, C.; Chaudret, B.; Devillers, J.; Poilblanc, R. *Organometallics* **1989**, *8*, 1308. (c) Paciello, R. R.; Manriquez, J. M.; Bercaw, J. E. *Organometallics* **1990**, *9*, 260.
(28) Borowski, A. F.; Sabo-Etienne, S.; Christ, M. L.; Donnadieu, B.; Chaudret, B. *Organometallics* **1996**, *15*, 1427.
(29) Kono, H.; Wakao, N.; Ito, K.; Nagai, Y. *J. Organomet. Chem.* **1977**, *132*, 53.
(30) Chung, G.; Arliguie, T.; Chaudret, B. *New J. Chem.* **1992**, *16*, 369.
(31) Gusev, D. G.; Kuhlman, R.; Rambo, J. R.; Berke, H.; Eisenstein, O.; Caulton, K. G. *J. Am. Chem. Soc.* **1995**, *117*, 281.

**Table 5.** Relative Energies (kcal/mol) and Selected Geometrical Parameters (Å and deg) for the DFT/B3LYP Optimized Stationary Points in the $RuH_2Cl_2(PH_3)_2$ Model Complex (Basis Set B)

| | **4a** ($C_{2v}$) | **4b** ($C_{2v}$) | **4c** ($C_{2v}$) | **4d** ($C_1$) |
|---|---|---|---|---|
| Ru−H1 | 1.560 | 1.567 | 1.602 | 1.554 |
| Ru−H2 | 1.560 | 1.567 | 1.602 | 1.604 |
| Ru−Cl1 | 2.379 | 2.387 | 2.393 | 2.410 |
| Ru−Cl2 | 2.379 | 2.387 | 2.393 | 2.396 |
| Ru−P1 | 2.357 | 2.303 | 2.236 | 2.469 |
| Ru−P2 | 2.357 | 2.303 | 2.236 | 2.227 |
| H1−H2 | 1.414 | 2.655 | 2.811 | 2.567 |
| P1−Ru−P2 | 179.6 | 112.3 | 103.3 | 140.2 |
| H1−Ru−H2 | 53.9 | 115.8 | 122.6 | 108.8 |
| Cl1−Ru−Cl2 | 149.0 | 90.2 | 87.9 | 158.1 |
| H1−Ru−Cl2 | 78.5 | 112.0 | 74.7 | 79.5 |
| H2−Ru−Cl1 | 78.5 | 112.0 | 74.7 | 106.6 |
| $\Delta E$ | 0.0 | 2.32 | 19.28 | 15.18 |

**4a** has $C_{2v}$ symmetry, with the two chloride and hydride ligands adopting cis positions in a common plane. The Ru−H distances are calculated to be a little shorter (0.061 Å) than those in **1a**, implying a reduced covalent radius for Ru(IV) compared to Ru(II), but the Ru−P distances change in the reverse order, being 0.046 Å greater in **4a** than in **1a**. Although the P−Ru−P angle in **4a** is almost exactly 180°, the H−Ru−H angle is notably acute (only 53.9°) and the Cl−Ru−Cl angle of 149.0° is closer to linearity than to 90°. One cannot argue convincingly that the large angle involving the chloride ligands in **4a** is due to steric repulsion between them, since in **4b**, which also has $C_{2v}$ symmetry, the Cl−Ru−Cl angle is only 90.2° and the Ru−Cl distances in **4a** and **4b** are almost identical. The most striking feature of **4b**, for which the two chloride and phosphine ligands occupy the same plane, is the position of the two hydride ligands; they are decidedly on the phosphine side of the coordination sphere, making an angle H−Ru−H of only 115.8°. A related isomer in which the two hydride ligands are in analogous positions but on the chloride side was also characterized computationally, but it is much less stable than **4b**, by 31 kcal/mol, and so it is not discussed further here. The structure of $RuH_2Cl_2(P^iPr_3)_2$, a complex which is closely related to **4**, was recently determined by X-ray diffraction;[13] the coordination about Ru in the solid state was described as a distorted square antiprism with two vacant sites in alternate positions in one square base. It is similar to that of **4b**, with P−Ru−P and Cl−Ru−Cl angles of 111.7 (calculated 112.3) and 84.3° (calculated 90.2°), respectively. However, there is a significant structural difference between **4b** and $RuH_2Cl_2(P^iPr_3)_2$; while the dihedral angle between the RuPP and RuClCl planes is 48° in $RuH_2Cl_2(P^iPr_3)_2$, those groups are coplanar in **4b**. As the steric bulk of the phosphine ligands in the experimental system is far greater than that of the simple model employed computationally, some structural differences might well be anticipated; Eisenstein and co-workers have reported that steric effects in the analogous Os complex favor a twisting of the OsPP plane relative to the OsClCl unit.[31] Isomer **4c** is related to **4a** in that the two chloride and two hydride ligands are coplanar but differs in that the P−Ru−P angle is only 103.3°.

We calculate the energy difference between **4a** and **4b** to be small, with **4a** more stable by 2.3 kcal/mol. We see no real contradiction in the detection in the solid state of an isomer which we have calculated to be slightly less stable than the global minimum, as packing effects could easily outweigh energy differences of only 2 kcal/mol. Because the energy difference between **4a** and **4b** is so small and because both were shown to be true minima by calculation of their vibrational frequencies, we would expect both to be present in detectable amounts in solution, consistent with the NMR behavior of **4** described above. We were not able to find computationally any other low-energy isomers of **4**. Isomer **4c** is sufficiently high in energy (19.3 kcal/mol above **4a**) that we do not expect it to be detectable by NMR spectroscopy in solution at room temperature. A nonsymmetric isomer **4d** was located ($C_1$ point group), which may be thought of as having essentially trans orientations of the hydride, chloride, and phosphine ligands, but it is substantially higher in energy than either **4a** or **4b** (15.2 kcal/mol above **4a**) and therefore unlikely to be present in detectable amounts in solution.

It is intriguing that the relative DFT energies of the isomers of **4** described here are rather different from those of the analogous Os system studied by Eisenstein, Caulton, and co-workers at the MP2 level of theory.[31] However, the differences may be more apparent than real; when MP2 energies are obtained for **4a** and **4b**, **4b** is slightly more stable, by 2.5 kcal/mol, i.e., just the reverse of the DFT result, even though the differences between DFT and MP2 geometrical parameters are insignificant. Since we have argued above that DFT results are more reliable than are the MP2 values for **1**, we presume that the same preference will still apply for **4**.

## Conclusion

We describe in this paper the high fluxionality of the bis(dihydrogen) complex $RuH_2(H_2)_2(PCy_3)_2$ (**1**). The origin of this fluxionality is both a rapid hydride−dihydrogen interconversion which cannot be blocked in Freons down to 143 K and a low barrier to rotation of coordinated dihydrogen (1.1 kcal/mol) as demonstrated by INS and studied computationally. Theoretical studies have shown that the bis(dihydrogen) complex **1** has three isomeric structures within an energy range of only 2 kcal/mol$^{-1}$ in agreement with the high fluxionality of this molecule. The geometry of the lowest energy isomer for **1** is unusual, since the two $H_2$ units and the hydride ligands are located in the same plane. Analysis of several dihydrogen complexes shows that the attractive cis effect[23] controls the geometrical preference. The barrier to rotation of dihydrogen is higher in the 16 electron iodo complex $RuHI(H_2)(PCy_3)_2$ (>ca. 3.5 kcal/mol$^{-1}$), but the interconversion on the NMR time scale remains also rapid at all accessible temperatures. For the corresponding chloro complex, we could demonstrate both the rapid equilibrium between the mono- and bis(dihydrogen) complexes $RuHCl(H_2)(PCy_3)_2$ and $RuHCl(H_2)_2(PCy_3)_2$ and the exchange between free and coordinated dihydrogen in $RuHCl(H_2)_2(PCy_3)_2$ which could be blocked at low temperature.

## Experimental Section

**General Considerations.** Microanalyses were performed at our laboratory's microanalyses service. Infrared spectra were obtained as Nujol mulls on a Perkin-Elmer 1725 FT-IR spectrometer. NMR spectra were recorded on a Bruker AC200 (at 200.13 MHz for $^1$H and at 81.015 MHz for $^{31}$P), while variable-temperature proton spectra were obtained by using Bruker AM250 (at 250 MHz for $^1$H and at 101.202 MHz for $^{31}$P) and AMX 500 (500 MHz; Freon experiments) spectrometers, all of these spectrometers operating on the Fourier transform mode. All manipulations were carried out in argon atmosphere by use of Schlenk techniques. Solvents were dried and distilled under dinitrogen and thoroughly degassed under argon before use. For the low-temperature NMR experiments, a mixture of deuterated Freons was synthesized by the literature methods.[17] According to the $^1$H and $^{13}$C NMR spectra, the mixture contained 9% $CDCl_3$, 45% $CDFCl_2$, and 45% $CDF_2Cl$. The solvent was stored in a stainless steel lecture bottle over basic alumina in order to remove water and acid impurities. The NMR

samples were prepared using vacuum methods as described previously.[32] In particular, pressure/vacuum valve NMR tubes (Wilmad, Buena, NY) were employed, which could easily be attached or removed from the vacuum line where they were filled with the solvent by vacuum transfer. The tubes were stored below 240 K. NMR line shape analyses were carried out using known methods.[18]

**Inelastic Neutron Scattering.** Inelastic neutron scattering studies were carried out on **1** and on $RuH(H_2)I(PCy_3)_2$ using the cold neutron time-of-flight spectrometers MIBEMOL and IN5 of the Laboratoire Léon Brillouin (CE Saclay, France) and Institut Laue-Langevin (Grenoble, France), respectively. Data were collected from 1.5 to 250 K using ~0.8 g of sample in which the $PCy_3$ ligands were deuterated for the ILL experiment.

**Theoretical Calculations.** The core electrons for both Ru and P were represented by pseudopotentials developed in Toulouse.[33] Sixteen electrons were treated explicitly for Ru (those corresponding to the atomic levels 4s, 4p, 5s, and 4d) and the five valence electrons for P. The basis used for Ru is of approximately triple-$\zeta$ quality, being specified as (8s,6p,6d)/[5s,5p,3d]. A double-$\zeta$ plus polarization basis was employed for P and Cl (d-type exponents 0.45 and 0.65, respectively). The spherical-harmonic representation of d-type functions was adopted. In our initial studies, a standard double-$\zeta$ basis was adopted for all hydrogen atoms; the resulting basis is indicated as "basis A". Most of the results we present were obtained with a larger basis "B", in which we added a p-type polarization function (exponent 0.9) to the six hydrogen atoms directly bound to ruthenium. Our best estimates of some relative energies were obtained with a still larger basis "C", in which a set of f-type functions (exponent 1.2) was added to the Ru basis. These single-point calculations were performed at higher levels of theory, such as Möller−Plesset perturbation theory to fourth order, treating single, double, and quadruple excitations (MP4SDQ), or coupled-cluster theory, treating explicitly single and double excitations together with a perturbative estimate of triple excitations (CCSD(T)), adopting geometries already obtained at a lower level of theory. All calculations were performed with the Gaussian 94 series of programs.[34]

**Materials.** $RuH_2(H_2)_2(PCy_3)_2$ (**1**) was prepared according to published methods.[6] $RuCl_3 \cdot 3H_2O$ was purchased from Johnson Matthey Ltd.; $PCy_3$ was purchased from Aldrich.

**Preparation of $RuH_2Cl_2(PCy_3)_2$ (4).** To a suspension of $RuH_2(H_2)_2(PCy_3)_2$ (250 mg; 0.38 mmol) in 10 mL of diethyl ether was added HCl(aq) (67 $\mu$L, 0.76 mmol). The reaction mixture was stirred for 1 h at room temperature, during which a pink-red solid precipitated. This was filtered off, washed with ether (8 × 4 mL), and dried in vacuo. Yield: 60%. Anal. Calcd for $RuC_{36}H_{68}Cl_2P_2$. C, 58.83; H, 9.34. Found: C, 58.51; H, 9.37.

**Acknowledgment.** The authors thank the Institut Laue-Langevin and the Laboratoire Léon Brillouin for the use of their facilities and Dr. Gerrit Coddens for assistance with data collection at the Laboratoire Léon Brillouin. Work at Los Alamos was supported by the office of Basic Energy Sciences, US Department of Energy. This work was supported by a PROCOPE grant. V.R. acknowledges a grant from the Ministerio de Educacion y Investigacion, J.T. acknowledges the Humboldt Association (Bonn, Germany), B.C. and S.S.-E. acknowledge the CNRS, and H.-H.L. acknowledges the Fonds der Chemischen Industrie (Frankfurt, Germany) for support. The theoretical part of this work was supported by the Centre National Universitaire Sud de Calcul, Montpellier, France (Project irs1013).

IC970697Y

(32) Limbach, H. H. *Dynamic NMR Spectroscopy in the presence of kinetic Hydrogen/Deuterium Isotope Effects*; NMR−Basic Principles and Progress, Vol. 23; Springer: Heidelberg, Germany, 1991; Chapter 2.

(33) Bouteiller, Y.; Mijoule, C.; Nizam, M.; Barthelat, J.-C.; Daudey, J. P.; Pélissier, M.; Silvi, B. *Mol. Phys.* **1988**, *65*, 2664.

(34) Frisch, M. J.; Trucks, G. W.; Schlegel, H. B.; Gill, P. M. W.; Johnson, B. G.; Robb, M. A.; Cheeseman, J. R.; Keith, T. A.; Petersson, G. A.; Montgomery, J. A.; Raghavachari, K.; Al-Laham, M. A.; Zakrewski, V. G.; Ortiz, J. V.; Foresman, J. B.; Cioslowski, J.; Stefanov, B. B.; Nanayakkara, A.; Challacombe, M.; Peng, C. Y.; Ayala, P. Y.; Chen, W.; Wong, M. W.; Andres, J. L.; Replogle, E. S.; Gomperts, R.; Martin, R. L.; Fox, D. J.; Binkley, J. S.; Defrees, D. J.; Baker, J.; Stewart, J. P.; Head-Gordon, M.; Gonzalez, C.; Pople, J. A. *Gaussian 94*; Gaussian, Inc.: Pittsburgh, PA, 1995.